Space Science and Engineering Cent
University of Wisconsin–Madison



# GEOSTATIONARY ATMOSPHERIC SOUNDER (GAS): SOUNDING RETRIEVAL PERFORMANCE STUDIES – YEAR 2

## A REPORT from the

## COOPERATIVE INSTITUTE FOR METEOROLOGICAL SATELLITE STUDIES

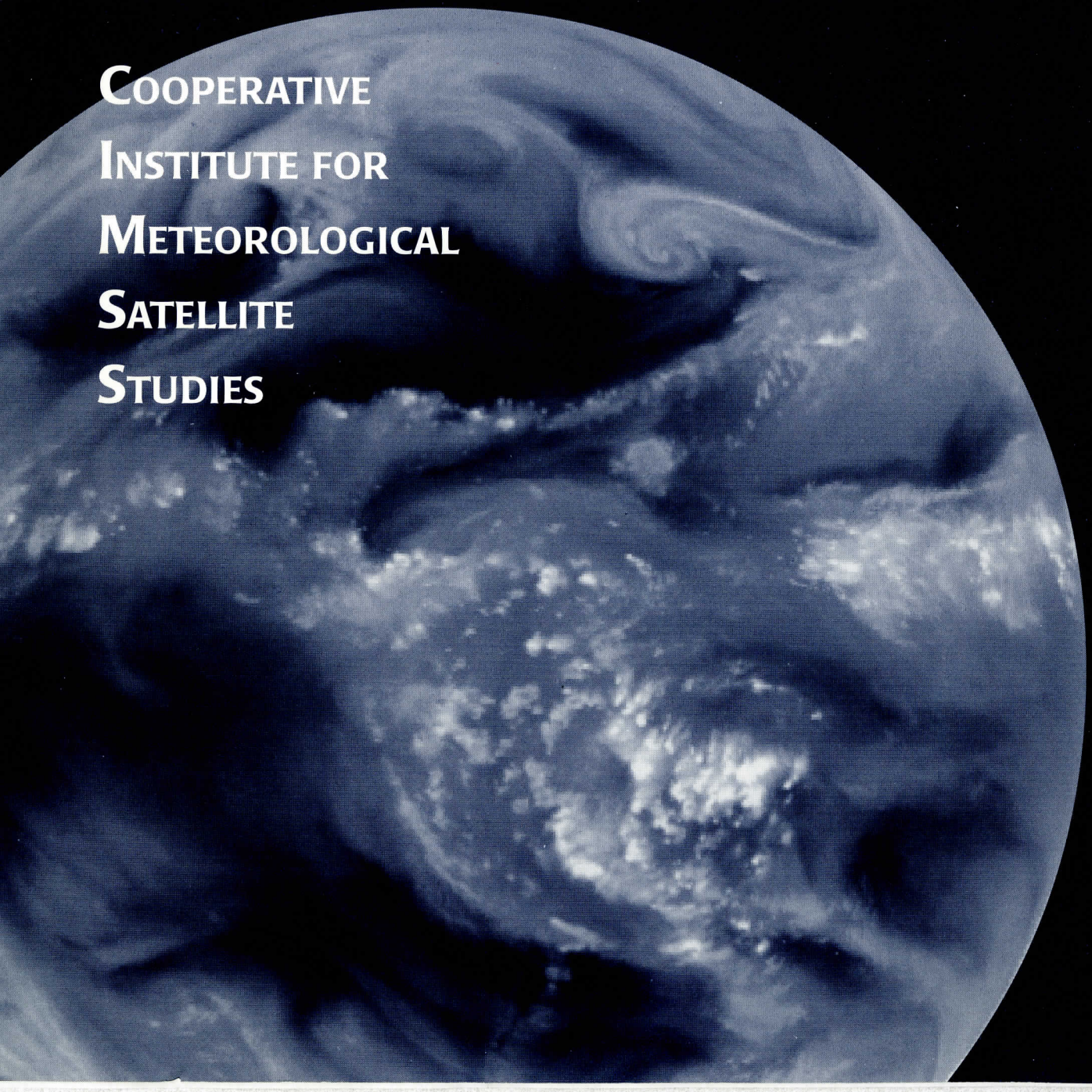

# GEOSTATIONARY ATMOSPHERIC SOUNDER (GAS): SOUNDING RETRIEVAL PERFORMANCE STUDIES – YEAR 2

Final Report to

AGS IR Sounder Program Office
Langley Research Center (LARC)
National Aeronautics and Space Administration (NASA)

For the Period
1 July 1998 to 31 May 1999

By

Allen H.L. Huang
Principal Investigator

The Cooperative Institute for Meteorological Satellite Studies (CIMSS)
Space Science and Engineering Center (SSEC)
University of Wisconsin-Madison
1225 West Dayton Street
Madison, Wisconsin 53706
608/263-5283
allenh@ssec.wisc.edu

June 1999

**Table of Contents**

**GEOSTATIONARY ATMOSPHERIC SOUNDER (GAS):**
**SOUNDING RETRIEVAL PERFORMANCE STUDIES - YEAR 2**

**Abstract**

The infrared Geostationary Atmospheric Sounder (GAS) will offer a major advance in capabilities for observing small spatial scale and short term temporal changes in the atmospheric state from space. It will provide quantitative measurements of variations in the distribution of water vapor, temperature and trace gases with high temporal resolution. The main tasks of this second year study was to conduct investigations of weather and chemistry sounding performance as a function of instrument design parameters. Specific tasks are classified: (1) to determine the optimal instrument configuration in terms of spectral resolution, spectral coverage, and signal to noise ratio for the sounding of thermodynamical and chemical gas concentration profiles; (2) to develop a physical based sounding retrieval algorithm to conduct performance analysis as described in (1); and (3) to define sensitivities of trace gases from the optimized instrument configuration for chemistry applications.

# 1. Introduction

The primary mission of the NASA MTPE sponsored Advanced Geosynchronous Studies (AGS) program is to conduct intensive studies to demonstrate the use of advanced new technologies and instruments on geosynchronous satellites to improve our current capabilities of monitoring the global weather, climate, and chemistry. The GAS mission, to be developed under AGS, is intended to demonstrate new space-based technology that is well suited for achieving the high temporal and spatial global coverage of cloud motion, water vapor transport, thermal and moisture vertical profiles, land and ocean surface temperature, and trace gas concentrations. The AGS technology demonstrations will show the capabilities of passive infrared observations from future NOAA geostationary operational sounders. These instruments will have much-improved spatial sampling and more rapid coverage than filter radiometer sounders. The proposed GAS characteristics are summarized in Table 1 and are used as the baseline instrument for the sounding retrieval performance study described below.

**Table 1. Summary of Proposed GAS Characteristics and Approach**

| | |
|---|---|
| Spatial Footprints | Nominal 9 km square, composed of 3x3 array subpixels allowing higher resolution options |
| Spatial Coverage | Nominal 9 km contiguous sampling in 42x42 groups, with other options allowed by 128x128, 3 km pixel array |
| Spectral Resolution | 0.1-1.0 $cm^{-1}$ unapodized<br>(5-0.5 cm Optical Path Difference) |
| Spectral Coverage (2 bands) | SW: 3.8-3.5 μm<br>MW: 3.5-12 μm |
| Telescope Aperture | 30.5 cm diameter (12 inches) |
| Interferometer | 5-8 cm beam diameter, Dynamically Aligned Plane-Mirror Michelson<br>(sized to keep angles small) |
| OPD Scan Drive<br>Scan rate | TBD<br>0.05-0.1 cm/s (Maximize consistent with readout) |
| OPD Sampling Reference | Stabilized Diode Laser |
| Detector Arrays | 128x128 elements with 60 μm pixel size<br>InSb SW and PV HgCdTe LW bands<br>With snapshot readout<br>At rates of at least 500 frames/sec |
| Detector Cooler/temperature | Stirling Cooler/68-80 K |
| Noise Performance | < 0.2 K Brightness Temperature at 280 K, for the nominal configuration and 60 sec dwell time |
| Onboard Processing | Subpixel processing to Effectively Field Widen Plus Data Compression |
| Mass | <100 kg |
| Power | <300 Watts |
| Size | <0.25 $m^3$ |
| Data Rate | TBD |

# 2. Instrument Simulation

GAS measurements are simulated using the baseline instrument configuration with variable spectral resolution, spectral coverage, and signal to noise ratio for global scenes. Figure 1 shows two brightness temperature spectra computed from a fast radiative transfer model for tropical atmospheric conditions from a 5 cm and 1 cm optical path difference (OPD) interferometer. The baseline spectral coverage from 3.8 micron (2631 1/cm) to 12 micron (833 1/cm) show absorption characteristics from carbon dioxide, ozone, water vapor, carbon monoxide, methane and nitrous oxide. The significant spectral resolving power difference owing to a 5 times OPD difference is clear. The trade off between the spectral resolving power and the accuracy of the derived retrieval parameters such as temperature, water vapor, and trace gases are demonstrated using similar spectra.

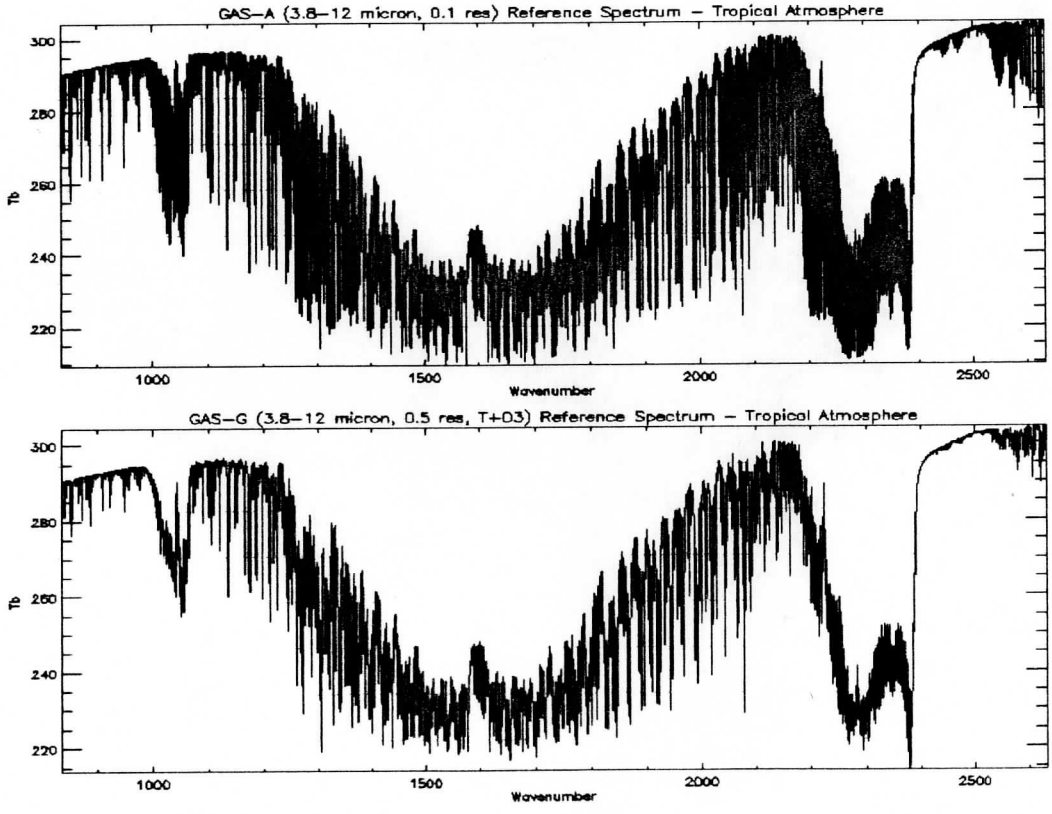


Figure 1. GAS brightness temperature spectra computed from tropical atmosphere for 5 and 1 cm OPD using GAS fast transfer model.

Chemistry applications will require that GAS spectral measurements have high sensitivity to trace gas constituents, such as ozone, methane, carbon monoxide, and nitrous oxide. Figure 2

shows 1976 U.S. standard atmosphere profiles used to analyze the measurement sensitivity at different spectral resolutions.

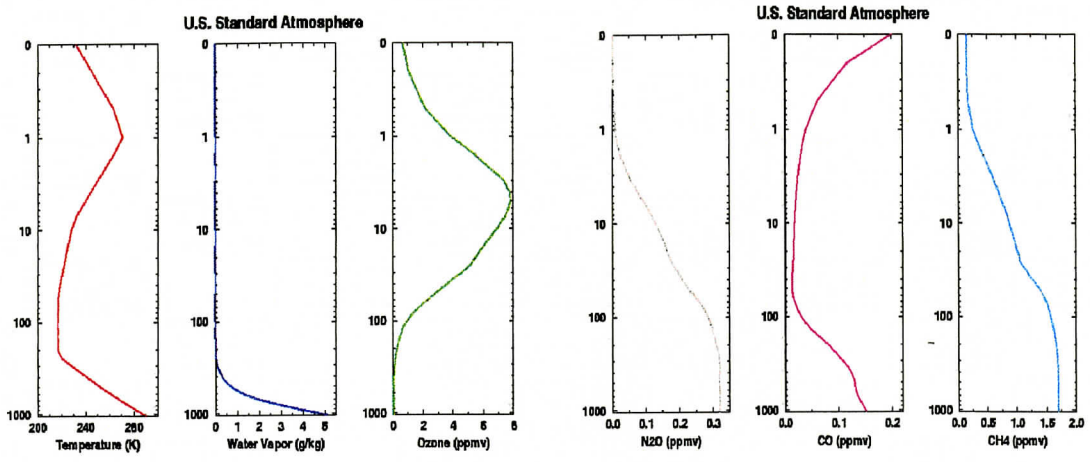


Figure 2. 1976 U.S. standard atmosphere temperature, water vapor and trace gas profiles.

Spectral differences are computed for four different spectral resolutions (0.05, 0.1, and 0.25 and 0.5 1/cm) for 20 % perturbations of the U.S. standard atmosphere trace gas profiles at prescribed level intervals. Figures 3 to 6 display the measurement sensitivity with a 20% increase in the trace gas concentrations of ozone, methane, carbon monoxide and nitrous oxide at the four spectral resolutions.

The signal to noise ratio does not necessarily favor higher spectral resolutions; since, the higher spectral resolution will result in higher measurement noise at the same measurement dwell time. Figures 3 to 6 demonstrate that resolutions close to 0.25 1/cm might be enough to obtain useful and accurate retrieval information for the total concentration of ozone, methane, nitrous oxide and carbon monoxide. Further study is required to define the optimal spectral resolution for obtaining trace gases' profiles and boundary layer gases' concentrations.

# 2. Instrument Performance Analysis

To support GAS instrument performance analysis, two retrieval approaches are developed. The two techniques are non-linear statistical regression analysis and non-linear physical retrieval. In the year one final report (Huang, 1998), the regression analysis is described and in this report the non-linear physical retrieval algorithm implementation is described.

## 3-1. Non-Linear Physical Retrieval Algorithm

The radiative transfer equation in linearized perturbation form for an atmosphere with two cloud layers may be written as (Huang, et.al., 1997)

$$\begin{aligned}\delta T_B = {} & (1-N_U-N_L)K^C(T_S,\ell_S)\delta T_S + N_U K(P_U)\delta P_U + K(N_U)\delta N_U \\ & + N_L K(P_L)\delta P_L + K(N_L)\delta N_L \\ & + \int_0^{P_S}\left\{(1-N_U-N_L)K^C(T,\ell)+N_U K^U(T,\ell)+N_L K^L(T,\ell)\right\}\delta T(P)dP \\ & + \int_0^{P_S}\left\{(1-N_U-N_L)K^C(q,\ell)+N_U K^U(q,\ell)+N_L K^L(q,\ell)\right\}\delta \ln q(P)dP \\ & + N_U K^U(T_{cd})\delta T_{cd}(P_U)+N_L K^L(T_{cd})\delta T_{cd}(P_L) \\ & + K(\varepsilon_{ir})\delta\varepsilon_{ir} + K(r_{ir})\delta r_{ir}, \end{aligned} \tag{3.1}$$

where,

| | |
|---|---|
| $\delta$ | is departure from initial (guess or background) state, |
| $\ell$ | is index of pressure level, |
| $\ell_S$ | is index of surface level, |
| $T_B$ | is GAS brightness temperature, |
| $N_U$ | is upper level cloud fraction, |
| $N_L$ | is lower level cloud fraction, |
| $P_U$ | is upper level cloud pressure, |
| $P_L$ | is lower level cloud pressure, |
| $P_S$ | is surface pressure, |
| $T_S$ | is surface temperature, |
| $T_{cd}$ | is cloud top temperature (either upper or lower), |
| $\varepsilon_{mw}$ | is microwave emissivity, |
| $\varepsilon_{ir}$ | is infrared emissivity, |
| $r_{ir}$ | is infrared reflectivity, |
| $K^C(T_S,\ell_S)$ | is clear Jacobian of skin temperature, |
| $K^C(T,\ell)$ | is clear Jacobian of temperature, |
| $K^C(q,\ell)$ | is clear Jacobian of water vapor, |
| $K^U(T,\ell)$ | is cloudy Jacobian of temperature (upper cloud), |
| $K^U(T_{cd})$ | is Jacobian of upper level cloud temperature, |
| $K^L(T,\ell)$ | is cloudy Jacobian of temperature (lower cloud), |

| | |
|---|---|
| $K^L(T_{cd})$ | is Jacobian of lower level cloud temperature, |
| $K^U(q,\ell)$ | is upper level cloud Jacobian of water vapor, |
| $K^L(q,\ell)$ | is lower level cloud Jacobian of water vapor, |
| $K(P_U)$ | is Jacobian of upper cloud top pressure, |
| $K(N_U)$ | is Jacobian of upper cloud fraction, |
| $K(P_L)$ | is Jacobian of lower cloud top pressure, |
| $K(N_L)$ | is Jacobian of lower cloud fraction, |
| $K(\varepsilon_{ir})$ | is Jacobian of infrared emissivity, |
| $K(r_{ir})$ | is Jacobian of infrared reflectivity. |

Equation (3.1) can be written in a more compact form as,

$$\delta y = K\delta x, \tag{3.2}$$

where $\delta y = \delta T_B$. The Jacobian, K, is a matrix containing the Jacobians in (3.1),

$$\mathrm{K} = [\ K^C(T_S,\ell_S)\ \ K(P_U)\ \ K(N_U)\ \ \ldots\ \ K(r_{ir})\ ],$$

and $\delta x$ is a vector of the variables to be retrieved,

$$\delta x = [\ \delta T_S\ \ \delta P_U\ \ \delta N_U\ \ \ldots\ \ \delta r_{ir}\ ]^T.$$

**Marquardt-Levenberg Iteration**

We wish to determine a solution, $\delta x$, to the nonlinear problem given in (3.2). If we assume that the forward model is a general function of the state vector, the measurement error is Gaussian and there is a prior estimate with a Gaussian error we may consider the maximum likelihood approach. With this approach, the goal is to select the most likely state, meaning the one for which P(**x**|**y**) is maximum, from an ensemble described by a probability density function. The probability density function for the maximum likelihood method is given by,

$$J(x) = (x - x_b)^T S_b^{-1}(x - x_b) + (y - F(x))^T S^{-1}(y - F(x)). \tag{3.3}$$

Where, x is the state vector, $x_b$ is the initial state and $S_b$ is its expected error covariance matrix. $S$ is the expected covariance of the combined measurement and forward model error, y is a vector of brightness temperature measurements, and F(x) is a vector of brightness temperatures calculated by the forward model.

To find the maximum likelihood state, the derivative of (3.3) with respect to x is set to zero. The resultant equation must be solved numerically. The GAS retrieval algorithm uses a hybrid nonlinear Newtonian iteration scheme, termed the Marquardt-Levenberg method, to accomplish this. This method incorporates the inverse Hessian method and method of steepest descent. The method was initially developed by Marquardt who, following the earlier work of Levenberg, found a way of combining the two approaches. The Marquardt-Levenberg method is formulated as

$$x_{n+1} = x_n - \left[\nabla^2 J(x_n) + \gamma I\right]^{-1} \nabla J(x_n), \tag{3.4}$$

where $\gamma$ is a parameter used to control the rate of convergence, $J(x_n)$ is the probability density function defined in (3.3) and $x_n$ and $x_{n+1}$ are the previous and current solutions respectively. If $\gamma \to 0$, this method tends to the inverse Hessian method, and if $\gamma \to \infty$ it tends to the method of steepest descent with a small step size. For each iteration, a value of $\gamma$ is determined and used in the next iteration to enable a weighting of the method of steepest descent when the retrieval is far from the solution, and a weighting of the inverse Hessian method when the prior retrieval is near the solution.

Therefore, the maximum likelihood solution for (3.2) using Marquardt-Levenberg iteration is given by,

$$x_{n+1} = x_b + (K_n^T S^{-1} K_n + S_b^{-1} + \gamma I)^{-1} [K_n^T S^{-1}((y - F(x_n)) + K_n(x_n - x_b)) + \gamma I(x_n - x_b)], \tag{3.5}$$

where all variables are defined as before.

**Eigenvector Transformation**

Because of the vertical correlation of temperature and water vapor at discrete levels in the atmosphere, it is possible to choose a small set of empirical orthogonal functions (EOFs) from which the atmospheric profiles can be reconstructed. The primary advantage of this method is that it significantly reduces the number of unknown variables in the retrieval algorithm. This means that the unknown state vector, $\delta x$, can be expressed in terms of EOFs as

$$\delta x = \varphi \hat{x},$$

where $\varphi$ is a matrix containing eigenvectors and $\hat{x}$ is a vector of expansion coefficients. In our particular situation the $\varphi$ matrix consists of the 15 temperature and water vapor eigenvectors with the largest eigenvalues. Therefore, (3.2), (3.3) and (3.4) may be equivalently written as

$$\delta y = K\varphi\hat{x},$$
$$\hat{J}(\hat{x}) = \hat{x}^T\varphi^T S_b^{-1}\varphi\hat{x} + (y - F(x))^T S^{-1}(y - F(x)),$$
$$\hat{x}_{n+1} = \hat{x}_n - \left[\nabla^2 J(\hat{x}_n) + \gamma I\right]^{-1}\nabla J(\hat{x}_n).$$

Setting the derivative of the transformed maximum likelihood solution to zero and substituting into the Marquardt-Levenberg iterative solution gives,

$$\hat{x}_{n+1} = \hat{x}_b + (\varphi^T K_n^T S^{-1} K_n\varphi + \gamma\lambda^{-1})^{-1}[\varphi^T K_n^T S^{-1}((y - F(x_n)) + K_n\varphi(\hat{x}_n - \hat{x}_b)) + \gamma\lambda^{-1}(\hat{x}_n - \hat{x}_b)]. \quad (3.6)$$

The quantities used retain their same meaning as before with two exceptions. First, the overhat on the state vector x indicates the solution is in eigenspace and not in physical space. Also the $\gamma\lambda^{-1}$ matrix still controls the rate of convergence as the gamma matrix does in (3.5). However, in eigenspace we can manipulate the eigenvalues associated with the EOFs to control convergence and maintain scaling between different physical quantities. The $\gamma\lambda^{-1}$ matrix consists of the 15 largest temperature eigenvalues and the six largest water vapor eigenvalues. The advantage of using EOFs within the retrieval algorithm is now evident: the dimensions of the matrix $\left(\varphi^T K_n^T S^{-1} K_n\varphi + \gamma\lambda^{-1}\right)$ to be inverted has been reduced from 156x156 in (3.5) to 42x42, which not only significantly reduces processing time and the number of unknown variables but also improves the stability of the retrieval.

**Convergence Criteria**

Each iteration of (3.6) requires the application of a convergence test to determine whether the solution is convergent or not. The $\gamma\lambda^{-1}$ matrix may then be adjusted based on the result of the convergence test. The convergence test applied to the Marquardt-Levenberg iteration determines the fit between the measurements and solution in terms of the "distance" between two consecutive solution sets,

$$\hat{d}_{n+1} = (\hat{x}_{n+1} - \hat{x}_n)^T (\varphi^T K_n^T S^{-1} K_n \varphi + \gamma\lambda^{-1})^{-1} (\hat{x}_{n+1} - \hat{x}_n), \tag{3.7}$$

with $\hat{d}_{n+1}$ being the "distance" between eigensolutions $\hat{x}_{n+1}$ and $\hat{x}_n$. If $\hat{d}_{n+1} < \hat{d}_n$, meaning the solution is converging, the $\gamma\lambda^{-1}$ elements are decreased and the state vector solution is updated. However, for the divergent solution $\hat{d}_{n+1} \geq \hat{d}_n$, the $\gamma\lambda^{-1}$ elements are increased and the iteration is repeated with the **same** state vector x that was used in the previous iteration.

Each convergent iteration of (3.6) also requires a conversion of the eigensolution back into physical space so that a brightness temperature residual test may be performed. The purpose of this second convergence test is to avoid overfitting the measured brightness temperatures. Once the infrared and microwave residuals reach a certain predetermined threshold, the solution is deemed satisfactory and iteration stops. The brightness temperature residuals are calculated as,

$$res_{n+1} = \sum_{i=1}^{nchan} (y - F(x_{n+1}))^2 / nchan . \tag{3.8}$$

**Computation of Jacobian K**

This section describes the calculation of the GAS Jacobians used in the retrieval algorithm. Variables used in this section retain their same meaning as before unless otherwise noted.

**Definition of Common Quantities**

This section groups together those quantities which appear in more than one of the following sections.

| | |
|---|---|
| B | is the Planck function, |
| R | is radiance, |
| ε | is emissivity, |
| $\beta(\ell) = \frac{\partial B / \partial T(\ell)}{\partial R / \partial T_B}$ | is the beta term, |
| $\tau$ | is total transmittance, |
| $\tau_d$ | is dry transmittance, |
| $\tau_w$ | is wet transmittance, |
| $\tau_o$ | is ozone transmittance, |

$\tau^*(\ell) = \frac{\tau_s \tau_s}{\tau\ (\ell)}$ is total transmittance product,

$\tau_d^*(\ell) = \frac{\tau_{d,s} \tau_{d,s}}{\tau_d(\ell)}$ is dry transmittance product,

$\tau_w^*(\ell) = \frac{\tau_{w,s} \tau_{w,s}}{\tau_w(\ell)}$ is wet transmittance product,

$\tau_o^*(\ell) = \frac{\tau_{o,s} \tau_{o,s}}{\tau_o(\ell)}$ is ozone transmittance product.

These subscripts have the following definition when used with these quantities,

| | |
|---|---|
| s | is surface level, |
| U | is level of upper cloud, |
| L | is level of lower cloud. |

**Jacobian of Skin Temperature**

The GAS Jacobian of skin temperature is defined as,

$$K^C(T_S, \ell_S) = \beta_S \varepsilon_{ir,S} \tau_S \,. \tag{3.9}$$

**Jacobian of Temperature Profile**

The GAS temperature Jacobian for clear conditions is,

$$K^C(T,\ell) = \beta(\ell)\left\{\tau_w(\ell)\tau_o(\ell)d\tau_d(\ell) + r_{ir}\tau_w^*(\ell)\tau_o^*(\ell)d\tau_d^*(\ell)\right\} \quad \text{for } 1 \le \ell \le \ell_S \tag{3.10}$$

where,

$$d\tau_d(\ell) = \begin{Bmatrix} 1-\tau_d(\ell) & ,\ell = 1 \\ \tau_d(\ell-1) - \tau_d(\ell) & ,2 \le \ell \le \ell_S \end{Bmatrix}$$

$$d\tau_d^*(\ell) = \begin{Bmatrix} 1-\tau_d^*(\ell) & ,\ell = 1 \\ \tau_d^*(\ell-1) - \tau_d^*(\ell) & ,2 \le \ell \le \ell_S \end{Bmatrix}.$$

The GAS temperature Jacobian for cloudy conditions is,

$$K^U(T,\ell) = \beta(\ell)\left\{\tau_w(\ell)\tau_o(\ell)d\tau_d(\ell) - (1-\varepsilon_U)\tau_{w,U}^*(\ell)\tau_{o,U}^* d\tau_{d,U}^*(\ell)\right\} \quad \text{for } 1 \le \ell \le \ell_U,$$

$$K^L(T,\ell) = \beta(\ell)\left\{\tau_w(\ell)\tau_o(\ell)d\tau_d(\ell) - (1-\varepsilon_L)\tau_{w,L}^*(\ell)\tau_{o,L}^* d\tau_{d,L}^*(\ell)\right\} \quad \text{for } 1 \le \ell \le \ell_L, \tag{3.11}$$

for the upper and lower cloud levels. The Jacobian for cloud top temperature is,

$$K^U(T_{cd}) = \varepsilon_U \tau_U \beta_U \quad \text{and} \quad K^L(T_{cd}) = \varepsilon_L \tau_L \beta_L . \tag{3.12}$$

The combined GAS temperature Jacobian is,

$$\begin{aligned} K(T,\ell) &= (1 - N_U - N_L) K^C(T,\ell) + N_U K^U(T,\ell) + N_L K^L(T,\ell) \\ &\quad + K^U(T_{cd}) + K^L(T_{cd}) . \end{aligned} \tag{3.13}$$

**Jacobian of Water Vapor Profile**

The GAS water vapor Jacobian for clear conditions is,

$$\begin{aligned} K^C(q,\ell) = \Bigg\{ & (T_s - T_a)\varepsilon_{ir,s}\tau_s\beta_s + \frac{2C_r\tau_s^2}{\partial R / \partial T_B} - 2(1-\varepsilon_{ir,s})\int_0^{P_s} \beta(\ell)\tau^*(\ell)\frac{\partial T}{\partial p}\,dp \\ & + \int_{P_{100}}^{P_s} \beta(\ell)[\tau(\ell) + (1-\varepsilon_{ir,s})\tau^*(\ell)]\frac{\partial T}{\partial p}\,dp \Bigg\} \frac{\partial \ell n \tau_w}{\partial p} \qquad \text{for } 1 \le \ell \le \ell_S , \end{aligned} \tag{3.14}$$

where $T_s$ and $T_a$ are skin and surface air temperature respectively, and

$C_r = 2.16x10^{-5}\pi\cos\theta\, r_{ir} B(T_{sun})$ where $\theta$ is the viewing angle and $T_{sun}$ is 5600° K.

The GAS water vapor Jacobian for cloudy conditions is,

$$\begin{aligned} K^U(q,\ell) = \Bigg\{ & (T_s - T_a)\varepsilon_{ir,U}\tau_U\beta_U + \frac{2C_r\tau_U^2}{\partial R / \partial T_B} - 2(1-\varepsilon_{ir,U})\int_0^{P_U} \beta(\ell)\tau^*(\ell)\frac{\partial T}{\partial p}\,dp \\ & + \int_{P_{100}}^{P_U} \beta(\ell)[\tau(\ell) + (1-\varepsilon_{ir,U})\tau^*(\ell)]\frac{\partial T}{\partial p}\,dp \Bigg\} \frac{\partial \ell n \tau_w}{\partial p}, \qquad \text{for } 1 \le \ell \le \ell_U \\ K^L(q,\ell) = \Bigg\{ & (T_s - T_a)\varepsilon_{ir,L}\tau_L\beta_L + \frac{2C_r\tau_L^2}{\partial R / \partial T_B} - 2(1-\varepsilon_{ir,L})\int_0^{P_L} \beta(\ell)\tau^*(\ell)\frac{\partial T}{\partial p}\,dp \\ & + \int_{P_{100}}^{P_L} \beta(\ell)[\tau(\ell) + (1-\varepsilon_{ir,L})\tau^*(\ell)]\frac{\partial T}{\partial p}\,dp \Bigg\} \frac{\partial \ell n \tau_w}{\partial p} \qquad \text{for } 1 \le \ell \le \ell_L . \end{aligned} \tag{3.15}$$

For cloudy conditions, $T_s$ is the cloud top temperature and $T_a$ is the air temperature at the closest discrete level to the cloud top.

The combined GAS water vapor Jacobian is,

$$K(q,\ell) = (1 - N_U - N_L)K^C(q,\ell) + N_U K^U(q,\ell) + N_L K^L(q,\ell) \tag{3.16}$$

**Jacobian of Cloud Top Pressure**

The GAS Jacobian of cloud top pressure for the upper and lower cloud is,

$$K(P_U) = \frac{R_{\ell_U - 1} - R_{\ell_U + 1}}{\ell n \Delta p \, \partial R / \partial T_B},$$
$$K(P_L) = \frac{R_{\ell_L - 1} - R_{\ell_L + 1}}{\ell n \Delta p \, \partial R / \partial T_B}, \tag{3.17}$$

where,

| | |
|---|---|
| $R_{\ell_U - 1}$ | is radiance at first discrete level above upper cloud top, |
| $R_{\ell_U + 1}$ | is radiance at first discrete level below upper cloud top, |
| $R_{\ell_L - 1}$ | is radiance at first discrete level above lower cloud top, |
| $R_{\ell_L + 1}$ | is radiance at first discrete level below lower cloud top, |
| $\Delta p$ | is pressure difference between discrete levels. |

**Jacobian of Cloud Fraction**

The GAS Jacobian of cloud fraction for the upper and lower clouds is,

$$K(N_U) = \frac{R_{U,cld} - R_{U,clr}}{\partial R / \partial T_B},$$
$$K(N_L) = \frac{R_{L,cld} - R_{L,clr}}{\partial R / \partial T_B}, \tag{3.18}$$

where,

| | |
|---|---|
| $R_{U,cld}$ | is cloudy radiance for the upper cloud, |
| $R_{U,clr}$ | is clear radiance for the upper cloud, |
| $R_{L,cld}$ | is cloudy radiance for the lower cloud, |
| $R_{L,clr}$ | is clear radiance for the lower cloud. |

## 3-2. Baseline System Performance Analysis

GAS baseline system performance is conducted by using statistical and physical retrieval algorithms described in the 1998 final report and in section 3-1 of this report. The sensitivity of trace gases' profiles, and the accuracy of temperature and water vapor are presented in the following sections.

### 3-2-1. Trace Gases' Sensitivity Analysis – Unpolluted Case

Four trace gases are considered in the sensitivity analysis. GAS measurements are computed from unperturbed standard atmosphere trace gas profiles at four different spectral resolutions (0.05, 0.1, 0.25, and 0.5 1/cm). Perturbed GAS measurements for the four resolutions are also computed for the trace gases' profile with a concentration increase of 20 % in specific layers. Four distinct layers are classified, the layers are: stratospheric (0 to 200 mb); tropospheric (200 to 700 mb); boundary (700 to 1000 mb); and total (0 to 1000 mb). The differences between the unperturbed and perturbed, in terms of brightness temperature, are displayed in the following figures. Figure 3 shows GAS has excellent signal sensitivity for all spectral measurements at resolutions higher than 0.5 1/cm for all layers except the boundary layer under unpolluted standard ozone profile condition.

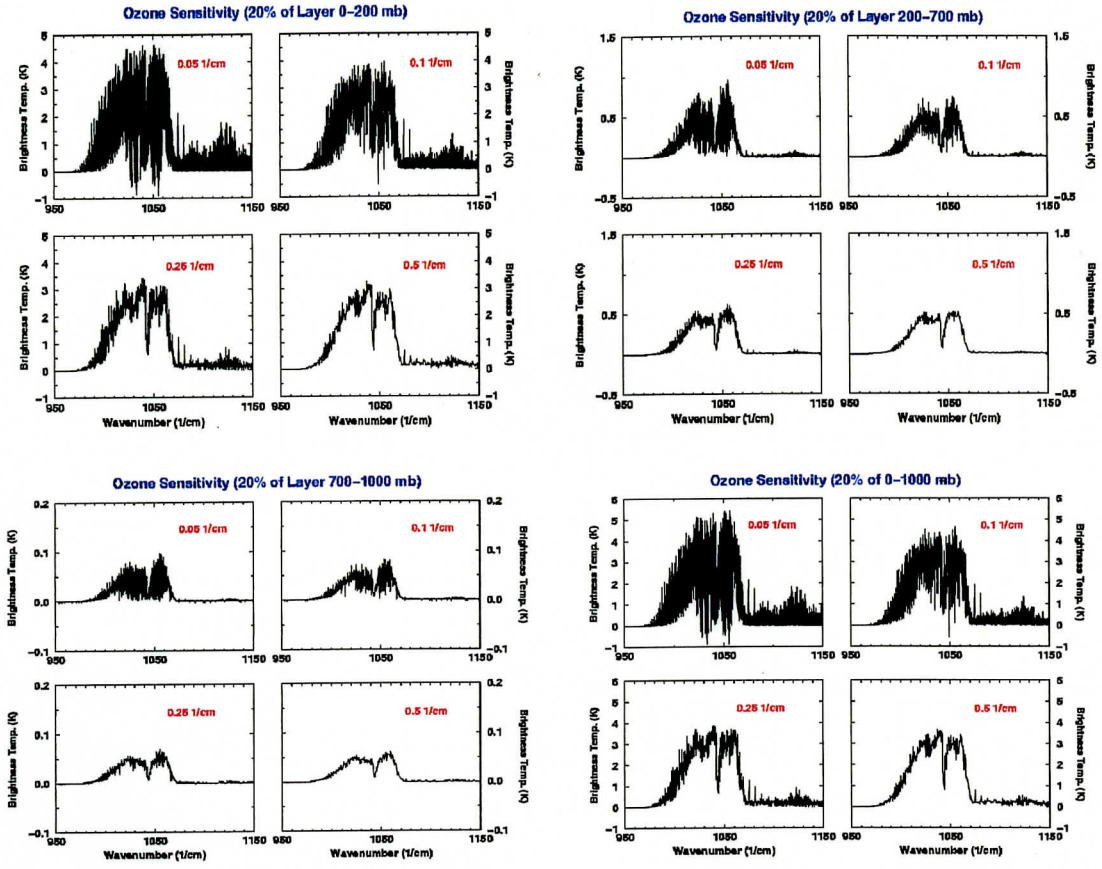


Figure 3, GAS measurements sensitivity to 20 % increases of layer mean ozone concentration, for four different layers, stratospheric (0 to 200 mb), tropospheric (200 to 700 mb), boundary (700 to 1000 mb), and total (0 to 1000 mb), and four different GAS spectral resolution, 0.05, 0.1, 0.25, and 0.5 1/cm.

Figure 4 shows GAS has good signal sensitivity for all spectral measurements at resolutions higher than 0.5 1/cm for all four layers except boundary layer under unpolluted standard methane profile condition.

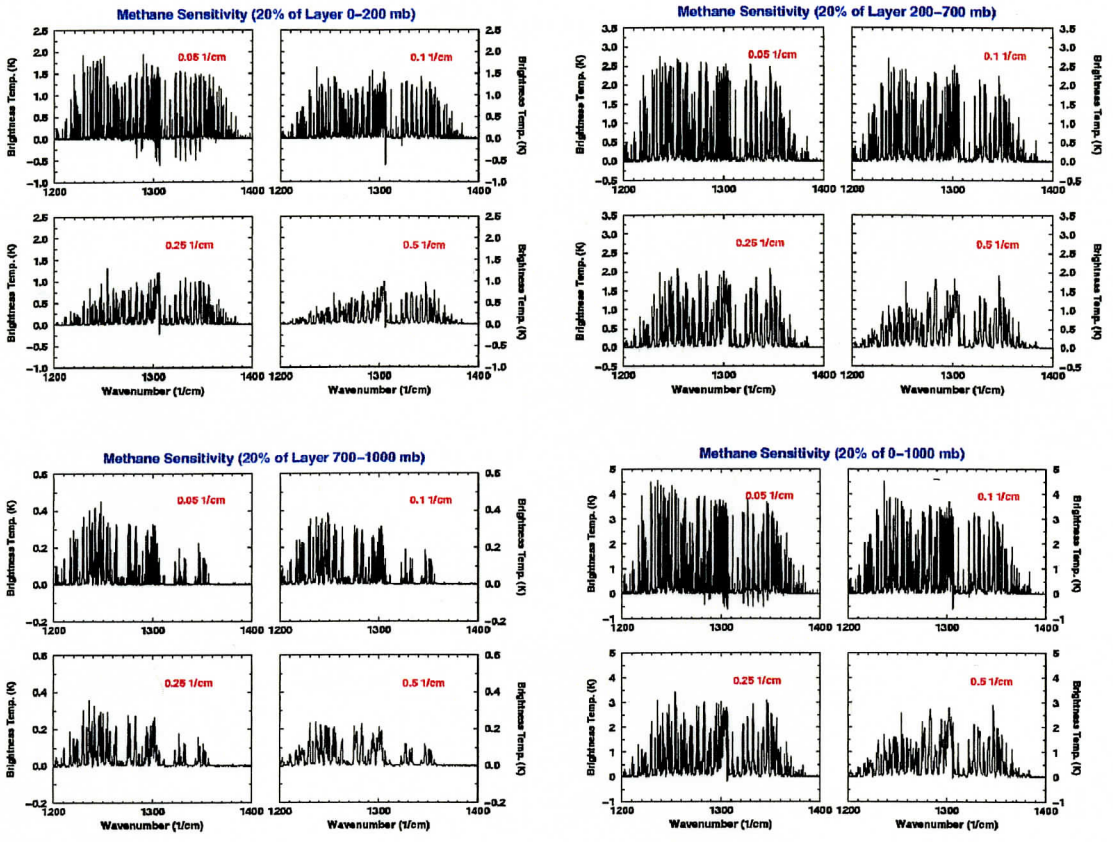


Figure 4, GAS measurements sensitivity to 20 % increases of layer mean methane concentration, for four different layers, stratospheric (0 to 200 mb), tropospheric (200 to 700 mb), boundary (700 to 1000 mb), and total (0 to 1000 mb), and four different GAS spectral resolution, 0.05, 0.1, 0.25, and 0.5 1/cm.

Figure 5 shows GAS has good signal sensitivity for all spectral measurements for all four layers under unpolluted standard nitrous oxide profile condition. Even 0.5 1/cm resolution measurements show significant signal for all four layers of nitrous oxide concentration changes.

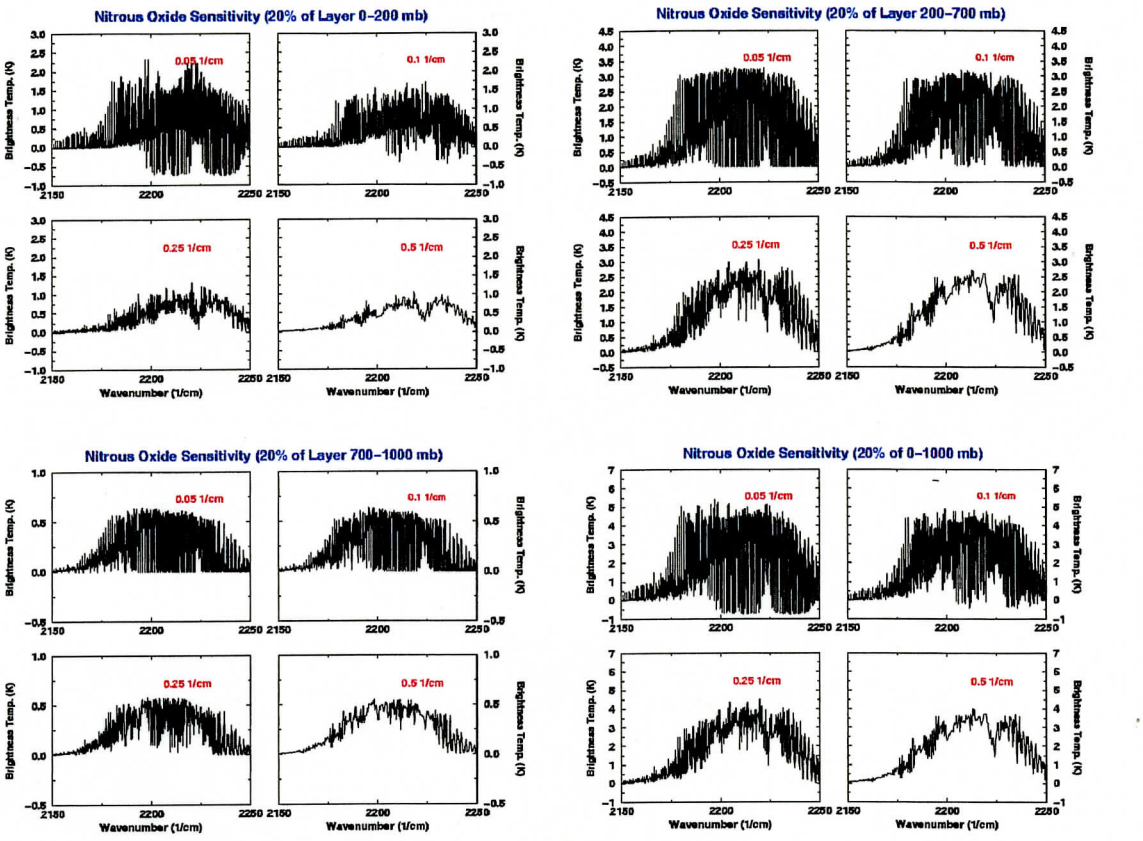


Figure 5, GAS measurements sensitivity to 20 % increases of layer mean Nitrous Oxide concentration, for four different layers, stratospheric (0 to 200 mb), tropospheric (200 to 700 mb), boundary (700 to 1000 mb), and total (0 to 1000 mb), and four different GAS spectral resolution, 0.05, 0.1, 0.25, and 0.5 1/cm.

Figure 6 shows GAS signal sensitivity for all spectral resolution measurements for all four layers under unpolluted carbon monoxide profile conditions. Resolutions higher than 0.25 1/cm are sensitive to all four layers of carbon monoxide concentration changes. Resolutions of 0.25 1/cm and lower can provide some sensitivities to tropospheric and total column concentration changes.

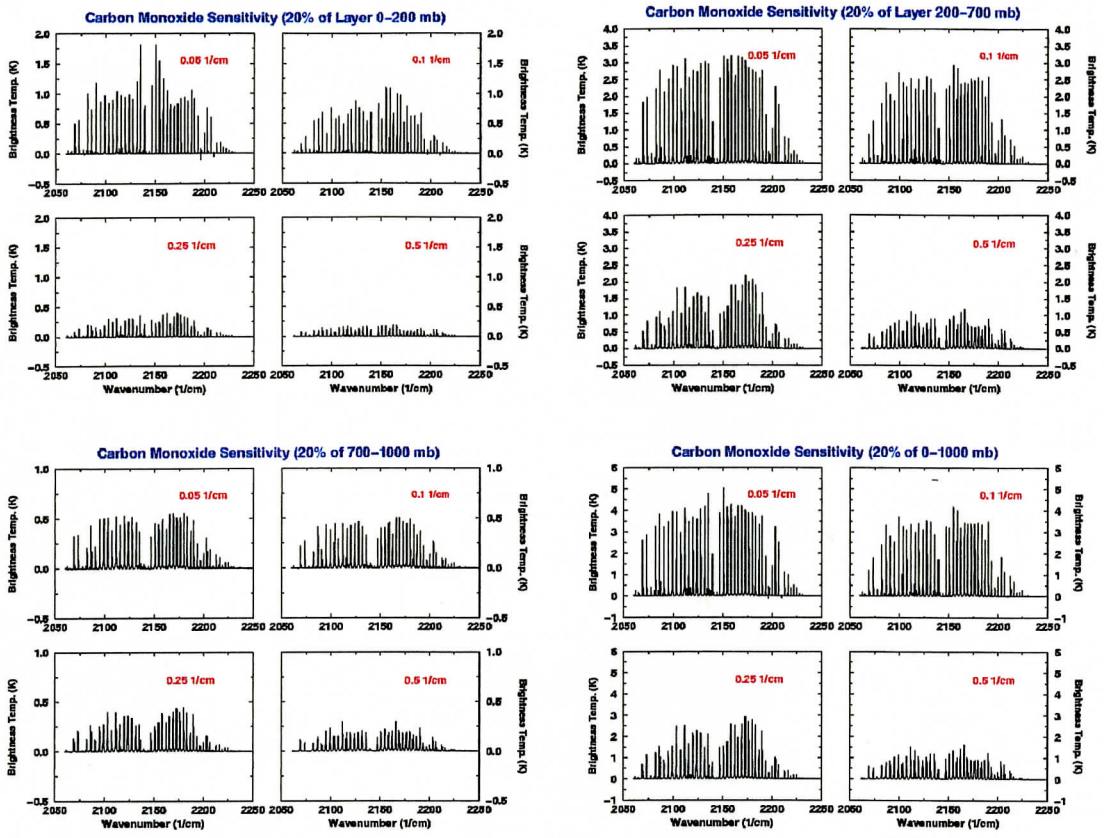


Figure 6, GAS measurements sensitivity to 20 % increases of layer mean carbon monoxide concentration, for four different layers, stratospheric (0 to 200 mb), tropospheric (200 to 700 mb), boundary (700 to 1000 mb), and total (0 to 1000 mb), and four different GAS spectral resolution, 0.05, 0.1, 0.25, and 0.5 1/cm.

The sum of signal to noise ratio (SNR) for trace gases are defined to quantify the GAS measurements sensitivity. Signal is defined as the brightness temperature difference between the standard and 20% increased layer concentration as shown in figures 3 to 6. GAS noise is assumed to be 0.25 K at 260 K for 0.25 1/cm resolution. Therefore, if the same dwell time for the five spectral resolutions is assumed, the noise factor will be 5.0 for 0.05 1/cm, 2.5 for 0.1 1/cm, 1 for 0.25 1/cm, 0.5 for 0.5 1/cm, and 0.25 for 1.0 1/cm. GAS spectral ranges for the computations of SNR sums are : 990-1070 1/cm for ozone; 1210-1360 1/cm for methane; 2080-2200 1/cm for carbon monoxide; and 2180-2250 for nitrous oxide. If the SNR value is smaller than one it is excluded in calculating the sums. Table 1 shows the sums of GAS SNR for five spectral resolutions, four trace gases and four vertical layers. For the stratospheric layer (0 to 200 mb), optimal measurement resolution for ozone is 0.05 or 0.1 1/cm, for methane it is 0.25 1/cm, for

nitrous oxide it is 0.25 1/cm, and for carbon monoxide resolutions higher than 0.25 1/cm provide a little sensitivity. For the tropospheric layer (200 to 700 mb), optimal resolution for ozone is 0.25 1/cm, for methane is 0.1 1/cm, for carbon monoxide is 0.05 or 0.1 1/cm, and for nitrous oxide is 0.05 1/cm. For the boundary layer (700 to 1000 mb), the optimal resolution for nitrous oxide is 0.1 or 0.25 1/cm. There are no sensitivity for ozone, methane, and carbon monoxide for the boundary layer. As for total column concentration, the optimal resolution for getting maximum sensitivity for ozone, methane, carbon monoxide, and nitrous oxide are 0.05 or 0.1 1/cm, 0.1 1/cm, 0.05 or 0.1 1/cm, and 0.05 1/cm, respectively.

| LAYER (mb) | RESOLUTION ($cm^{-1}$) | TRACE GASES | | | |
|---|---|---|---|---|---|
| | | $O_3$ | $CH_4$ | CO | $N_2O$ |
| 0-200 | 0.05 | 2466 | 22 | 1 | 29 |
| | 0.1 | 2456 | 146 | 7 | 317 |
| | 0.25 | 1825 | 212 | 10 | 323 |
| | 0.5 | 1127 | 145 | 0 | 226 |
| | 1.0 | 604 | 74 | 0 | 126 |
| 200-700 | 0.05 | 0 | 458 | 327 | 1903 |
| | 0.1 | 16 | 648 | 338 | 1772 |
| | 0.25 | 208 | 588 | 219 | 1252 |
| | 0.5 | 147 | 387 | 110 | 822 |
| | 1.0 | 81 | 212 | 48 | 455 |
| 700-1000 | 0.05 | 0 | 0 | 0 | 0 |
| | 0.1 | 0 | 0 | 14 | 211 |
| | 0.25 | 0 | 3 | 19 | 214 |
| | 0.5 | 0 | 0 | 2 | 147 |
| | 1.0 | 0 | 0 | 0 | 80 |
| 0-1000 | 0.05 | 2922 | 984 | 513 | 2887 |
| | 0.1 | 2868 | 1168 | 502 | 2640 |
| | 0.25 | 2123 | 977 | 311 | 1851 |
| | 0.5 | 1310 | 644 | 159 | 1202 |
| | 1.0 | 702 | 350 | 73 | 664 |

Table 1, sum of signal to noise ratio of GAS trace gases sensitive spectral regions for different part of atmosphere. Four spectral resolutions of GAS measurements are considered.

Table 2 summarizes the sensitivity results of table 1 using rankings of zero to 0. Where 10 means very good sensitivity that is achievable by GAS measurements for the assumed noise level and spectral resolution. Ranking of zero means GAS measurements cannot provide any significant sensitivity towards measuring the trace gases. Three means marginal measurement capability, six means fair measurement capability, and eight means good measurement capability.

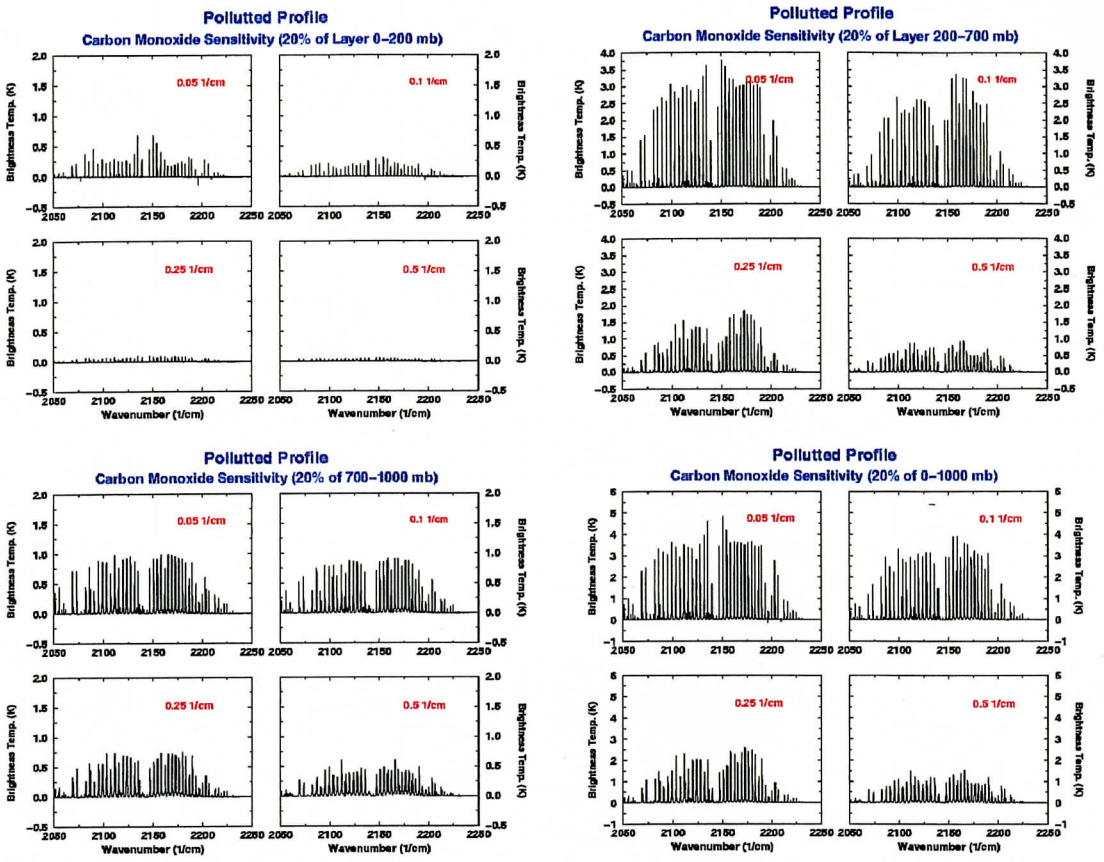


Figure 7, GAS measurements sensitivity to 20 % increases of layer mean polluted carbon monoxide concentration, for four different layers, stratospheric (0 to 200 mb), tropospheric (200 to 700 mb), boundary (700 to 1000 mb), and total (0 to 1000 mb), and four different GAS spectral resolution, 0.05, 0.1, 0.25, and 0.5 1/cm.

## 3-3. Spectral Resolution and Coverage Trade-off

Temperature and water vapor profile sounding performance is strongly related to the spectral resolution of GAS measurements. Three different sounding spectral resolutions are analyzed to see how the GAS measurements are related to the sounding accuracy. Figure 8 and 9 shows 605 global temperature and water vapor retrieval root mean square error (RMSE) as function of measurement spectral resolutions of 0. 25, 0.625 and 15 1/cm. Temperature and water vapor sounding at resolution of 0.625 1/cm can provide retrieval with better than 1 degree RMSE of 1 km layer mean temperature, and 10 to 15 % RMSE of 2 km layer mean water vapor. The 0.625 1/cm resolution seems to be able to provide enough sounding accuracy for Numerical Weather Prediction (NWP) and climate applications.

**GAS IR Sounder Trace Gases Sensitivity Rankings**

| | Stratospheric (0-200 mb) | Tropospheric (200-700 mb) | Boundary (700-1000 mb) | Total (0-1000 mb) |
|---|---|---|---|---|
| $O_3$ | 9 | 3 | 0 | 10 |
| $CH_4$ | 3 | 6 | 1 | 7 |
| CO | 2 | 4 | 1 | 5 |
| $N_2O$ | 4 | 8 | 3 | 10 |

**0 - Infeasible ; 3 – Marginal ; 6 – Fair**
**8 – Good ; 10 – Very Good**

Table 2, The sensitivity ranking of un-polluted U.S. standard profile conditions with 10 degree K surface air-skin temperature contrast and 20 % layer gas concentration changes.

## 3-2-2. Trace Gases Sensitivity Analysis – Polluted Case

Only the polluted Carbon monoxide profile is analyzed for GAS trace gas sensitivity study at this time. Figure 7 shows that the stratospheric layer has no sensitivity for any resolution. The boundary layer has less sensitive GAS measurement information than tropospheric and total column carbon monoxide. Spectral resolution dependency indicating 0.25 1/cm is essential but 0.1 1/cm greatly enhance the GAS measurements sensitivity.

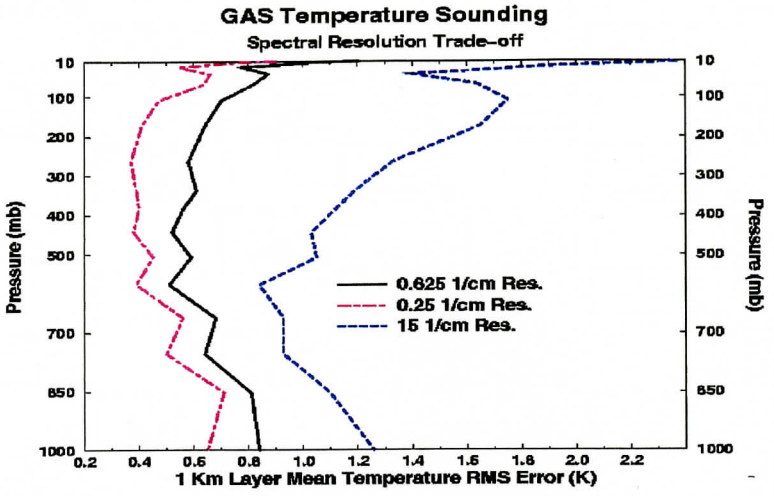


Figure 8, RMS error of 605 global retrieved temperature profile (60 S to 60 N) using 685-2510 1/cm GAS spectral measurements, NEdT of 0.25K at 250K and spectral resolutions of 0.625 1/cm, 0.25 1/cm, and 15 1/cm.

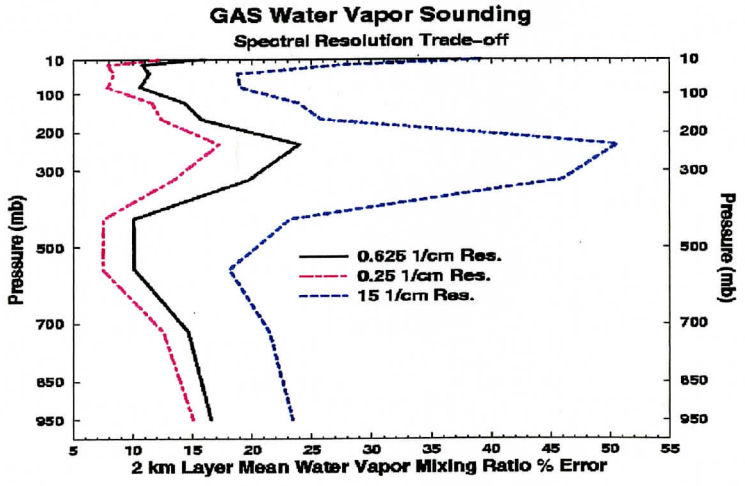


Figure 9, RMS error of 605 global retrieved water vapor profile (60 S to 60 N) using 685-2510 1/cm GAS spectral measurements, NEdT of 0.25K at 250K and spectral resolutions of 0.625 1/cm, 0.25 1/cm, and 15 1/cm.

Spectral coverage is also an important trade-off for GAS instrument design. The three spectral ranges analyzed are all coverage, (685-2510 1/cm), longwave and midwave coverage, (685-1600 1/cm), and, midwave and shortwave coverage, (1600-2510 1/cm). Figure 10 and 11 show the sounding performance using these three different spectral coverage measurements at the

same NEdT of 0.25 K at 250 K scene. In general, infrared measurements that cover shortwave to longwave have the best overall retrieval performance. Longwave infrared seems to have much more temperature information than shortwave infrared. Without longwave infrared measurements the sounding is greatly degraded. Shortwave only provides improvement of temperature at the boundary layer. However, accurate measurement of boundary layer temperature is very significant for NWP applications. Figure 10 and 11 demonstrate temperature and water vapor soundings for three spectral bands if GAS were to operate in a low resolution mode (15 1/cm resolution vs. 0.1 1/cm resolution for chemistry sounding mode). All coverage (685-2510 1/cm) GAS retrievals provide the best overall and useful temperature and water vapor soundings. Without the shortwave infrared spectral coverage(1600-2510 1/cm), GAS retrieval accuracy is degraded at all levels. Significant degradation for lowest few boundary layers demonstrates the utility of shortwave spectral information at this resolution. If longwave and part of midwave infrared (685-1600 1/cm) data are not available then the mid to upper level temperature retrieval accuracy is severely degraded, but not the layers near the surface. Again, this shows how longwave coverage is vital to accurate temperature soundings. Water vapor sounding accuracy of three different spectral coverage (685-2510; 685-1600 and 1600-2510 1/cm) shows similar characteristics to temperature soundings with less layer discrimination.

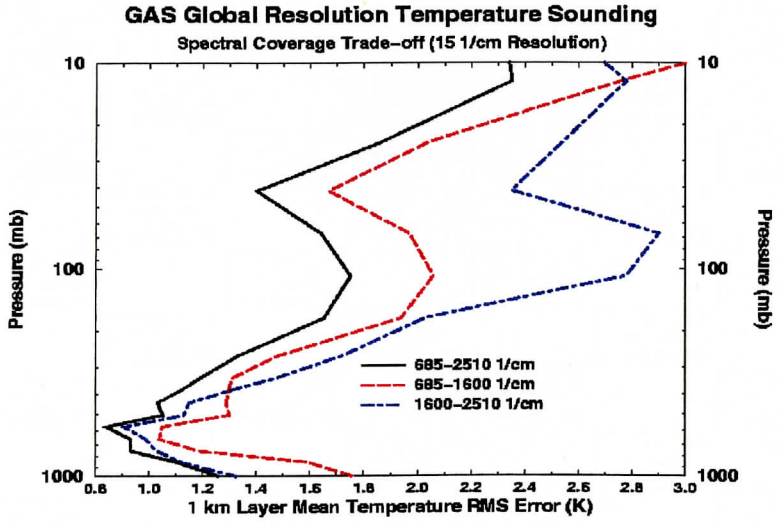


Figure 10, RMS error of 605 global retrieved temperature profiles (60 S to 60 N) using 15 1/cm spectral resolution GAS measurements, NEdT of 0.25K at 250K and spectral coverage of 685-2510, 685-1600, and 1600-2510 1/cm.

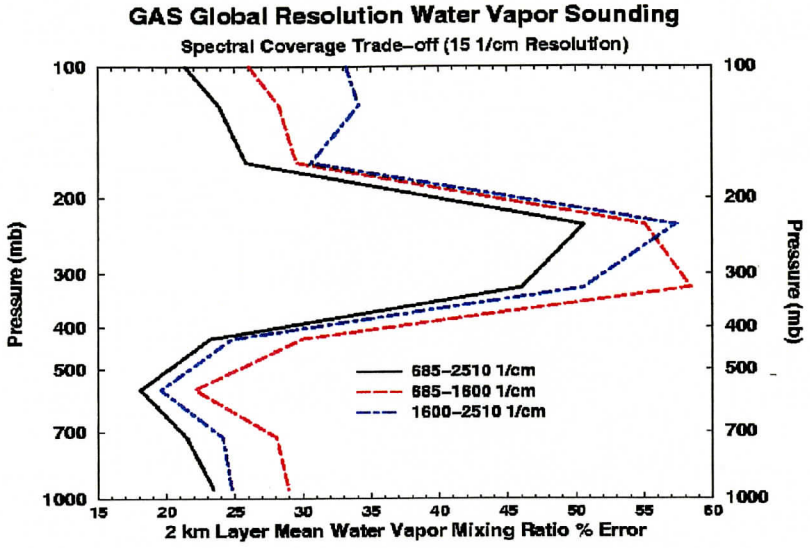


Figure 11, RMS error of 605 global retrieved water vapor profiles (60 S to 60 N) using 15 1/cm spectral resolution GAS measurements, NEdT of 0.25K at 250K and spectral coverage of 685-2510, 685-1600, and 1600-2510 1/cm.

Figure 12 and 13 is the same as figure 10 and 11 except using GAS measurements of 0.625 1/cm spectral resolution. Similar conclusion can be made for the spectral coverage affect on the temperature and water vapor sounding performances.

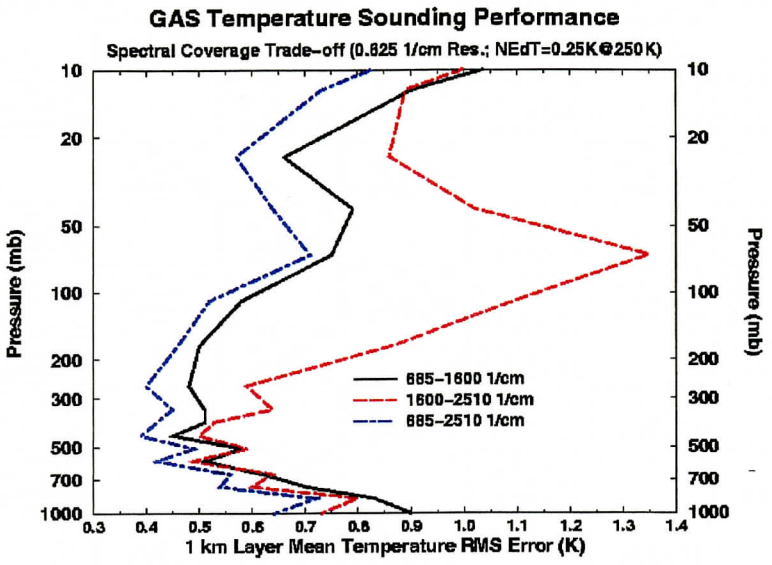


Figure 12, RMS error of 605 global retrieved temperature profiles (60 S to 60 N) using 0.625 1/cm spectral resolution GAS measurements, NEdT of 0.25K at 250K and spectral coverage of 685-2510, 685-1600, and 1600-2510 1/cm.

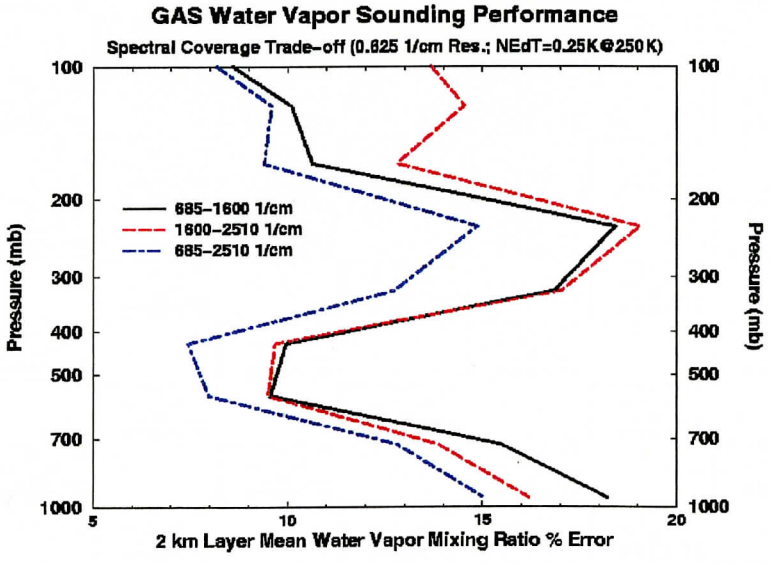


Figure 13, RMS error of 605 global retrieved water vapor profiles (60 S to 60 N) using 0.625 1/cm spectral resolution GAS measurements, NEdT of 0.25K at 250K and spectral coverage of 685-2510, 685-1600, and 1600-2510 1/cm.

# 4. Summary

Linear statistical and non-linear physical GAS retrieval algorithms are developed and ready to be used for an instrument design trade-off analysis. This analysis suggests GAS instrument configuration of 0.25 1/cm spectral resolution with noise of 0.25 K at 250 K scene temperature. This configuration will provide fair to very good sensitivity to unpolluted trace gases' retrieval for: stratospheric and total ozone; stratospheric, tropospheric and total methane; total carbon monoxide; and tropospheric and total nitrous oxide.

Trade-off studies of spectral resolution indicates 0.625 1/cm measurements are capable of providing sounding of 1 K and 15-20 % root mean square error of temperature and water vapor. Spectral coverage from shortwave to longwave infrared is very desirable, loss of any infrared bands will result in a degradation of the sounding performance. In the coming year, CIMSS will continue to support NASA Langley's efforts for sounding instrument in geostationary orbit sounding instruments. The support will include instrument design, data processing, algorithm development, and generation of products and applications. Algorithms developed under the two years GAS project can be used for other related programs. CIMSS will deliver a GAS related software system to Langley at the request of the GAS program manager.

# References

Huang, H.-L., W. L. Smith and M. S. Whipple, 1997 : Atmospheric Profile Retrievals Using Grating and Interferometer Infrared and Microwave Measurements. Fourier Transform Spectroscopy, Opt. Soci. of America, Feb 9-14, 1997, Santa Fe, New Mexico. P68-72.

Huang, H-L., 1998 : Geostationary Atmospheric Sounder (GAS): Sounding Retrieval Performance Studies – Year 1 final report. The Cooperative Institute for Meteorological Satellite Studies (CIMSS). 22pp.

UW AIRS Core Algorithm Development Science Documentation, 1996, UW-Madison.